Design of an Advance Microstrip Patch Antenna for Sub-6GHz Biomedical Applications

Bimal Raj Dutta
Electronics and Communication Engineering
Chandigarh University
Mohali, India

Balaka Biswas
Mechatronics Engineering
Chandigarh University
Mohali, India

***Abstract*—** Advance communication devices are taking an application-centric approach, and in the recent years, wearable accessories have integrated electronic devices. The paper presents the advance wearable circular patch antenna on a textile substrate - Felt. The designed antenna on textile substrate has an operating frequency range of Sub-6GHz (1-6GHz) with dimensions 48x48x5 mm^3 on a DGS ground structure. The proposed antenna offers a gain of 5.792 dBi and 5.325 dBi on free space at frequencies 3.545 GHz and 4.715GHz respectively. It has also been proposed for the detection of kidney stones for which an additional human body phantom has been created with the gain 0.404 and -4.49 dBi at 2.745 and 3.1GHz frequencies respectively. A SAR value of 1.54 W/kg has been obtained for 10g of tissue which is suitable for the human body. The proposed antenna has been designed and simulated with the help of CST Studio 2022. The described patch antenna will have a potential application in the fields of wearable technology, medical imaging, tumor detection, and WBAN biomedical applications,

Keywords— Circular Patch Antenna, Wearable, Sub-6GHz, Gain, Biomedical, Kidney Stone Detection

I. INTRODUCTION

Communication keeps people in a global community linked. In most wearable gadgets, the antenna and batteries are large and necessary components. Still, the wearable computer system's size and design have shrunk as electronic components have advanced recently. Because of this, the antennae have been made of cloth. Moreover, fabric-garment embedded antennas offer a production substitute for a range of rigid substrates [1]-[4]. Additionally, wearable textile systems can provide navigation, public safety, and tracking[5]-[9]. The need for flexible and wearable antenna devices has grown significantly in the last several years, as has the development of these devices. The development of implantable gadgets for a range of medical applications, including endoscopy, medical imaging, kidney stone detection, tumor detection, and more, is indicative of the wearable technology revolution. Along with WiMax, WLAN, WBAN, and other areas, wearable antennas have become essential components [10]-[15]. In these applications, microstrip patch antennas (MPAs) are the most widely utilized type of antenna. Its affordability, ease of fabrication, and portability owing to its light weight are the reasons behind this. All that makes up a MPA is a patch of dielectric material, like copper, positioned above ground on top of another dielectric substrate. Since the human body operates as a lossy platform for electromagnetic waves, a significant portion of those waves are absorbed into the body as heat and energy, making the MPA ideal for wearable or other biomedical applications.[16]-[20]

This paper uses the Sub-6 GHz because of its highly used application in its 5G spectrum and high data rates. Scientists are concentrating on Sub-6 GHz 5G mid-band spectrum since it is a highly deployable spectrum that can be used with the current 4G-LTE system's infrastructure. Many industries that demand fast data speeds, low latency, and consistent radiation patterns can benefit from the use of 5G technology [21]-[24]. Flexible electronics is one of the main industries that would profit greatly from the spread of 5G. Compact devices require an antenna with outstanding performance characteristics that is lightweight, flexible, and conformal. Due to the varying curvatures of the human body at different body areas, flexible antennas used in wireless body area networks (WBANs) must be extremely conformal.[25]-[28]

One of the most excruciating medical disorders that can affect a person is kidney stones. Kidney stones cause more than 500,000 people to visit the emergency room each year. The kidneys may be damaged as a result of kidney diseases that are not detected in their early stages. It is preferable to look into the problem in the first stage because kidney blockages can be dangerous. One of the pre-made lows that is widely used to identify renal problems is the ultrasonography machine [29]-[32]. Alterations in location and manifestation may be the cause of kidney morphological anomalies, such as kidney puffiness. In addition to kidney anomalies, tumor cells, stones, inborn abnormalities, urine interception, and particularly excruciating discomfort for the patient are possible consequences of kidney anomalies. Establishing the exact location of the kidney stone is crucial for surgical procedures. Low disparity, fleck din, and human body effect are characteristics of the ultrasonic machine [33]-[36]. Researching kidney anomalies follows, which involves some challenging work. So, the best option might be to use microwave imaging techniques.[37]-[41]

The work done in this paper is covered in greater depth in in the sections that follow. Section II examines and talks about the earlier research that was conducted on such wearable devices and biomedical applications. Section III discusses the suggested design of the antenna and how it is made compatible for the human body. Section IV presents the simulated results of the antenna proposed and is also presented in a tabular form. Section V gives us the comparison of achieved results from the previous studies along with the proposed work in this paper. Section VI summarizes and concludes the overall work done in this paper along with its future scope.

II. PREVIOUS LITERATURE STUDY

Several antennas has been designed in the past for fulfilling the purpose of wearable and biomedical applications. Few of those designs an their studies have been discussed in detail below along with their results.

The researchers simulate and build a wearable antenna with a flexible textile substrate in this study [42] and they also evaluate many aspects of antenna performance. The purpose of this research is to demonstrate a compact UWB antenna construction, measuring 20mm x 22mm x 1.07mm for the antenna. The anticipated dual-band antenna has a notable FBW of 103.50% in the UWB region, and its resonance frequencies are 4.450 and 8.750 GHz. The textile MPA that is being given here is a fantastic option for use as an on-body antenna for WBAN applications and wireless health device monitoring because it is small, robust, and flexible. "Jeans," a textile substrate used in this study, has a dielectric constant of 1.7. Figure 1 shows this proposed UWB antenna design.

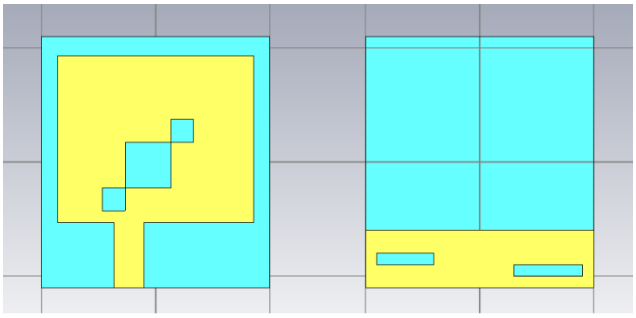

Fig.1 Layout of proposed antenna
a) Slotted Patch antenna, b) Partial Ground Structure

In this study [43], the researcher presents, a wearable microstrip patch antenna which is operational within the ISM bands of (2.4 -2.4835GHz). The research also consists of designing a body phantom of a human head for the purpose of detection of brain tumour using the software CST Studio Suite. The chosen substrate chosen is the FR-4 as it is the most low-cost and flexible material. The antenna designed achieved a return loss of -22.299 dB along with a directivity of 4.731 dBi at 2.424GHz. The SAR value calculated of the proposed antenna is found to be of 0.586 W/kg for a 10g tissue. A bandwidth of 1.6 GHz was also observed form the simulated results.

An implanted, miniaturized antenna device for biomedical applications is shown in another paper [44]. Internal and external patch antennas are two virtually similar patch antennas that make up the system. Both the inner and outside antennas are attached to the body in the same direction. The inner antenna is inserted into the body 2.00 mm. A 10.25 x 10.25 x 1.27 mm^3 implant-side antenna and an 11.1 x 11.11 x 1.27 mm^3 external antenna make up the antenna configuration. The suggested antenna designs showcased multiple resonant frequencies on ISM bands, specifically 915.0 MHz and 2450.0 MHz. The external and internal antennas achieve bandwidths of 2.38 to 2.47 GHz and 870 to 970 MHz, respectively, according to the computed -10.0 dB bandwidth using a triple layered human phantom.Medical treatment with the (SAR) has also been studied. There is good correspondence between the modeled and actual S11 parameters.

Another study [45] presents an adaptable textile substrate-based wearable antenna . The design consists of a 25x20x1 mm^3 low-profile textile-based UWB (3.1 - 10.6 GHz) antenna with a DGS construction. CST Studio Suite 2022 has been used to model design antenna performance characteristics. When employing a cotton substrate with a 1.6 dielectric constant, it provided a gain of 4.204 dBi at 5.11 GHz and 2.993 dBi at 7.39 GHz. The design antenna had a gain of 0.697 dBi, a return loss of -30.863 dB, and a 1.058 VSWR at 5.3125 GHz frequency, according to simulation tests conducted on a human body phantom. The planned antenna for 10g tissue has a SAR value of 1.64 W/kg, indicating that it is safe for human use. It was concluded that the designed MPA in this study was seen to be promising for applications such as medical imaging, tumour detection, wearable and other WBAN applications. The Figure below (Fig.2) shows the proposed antenna.

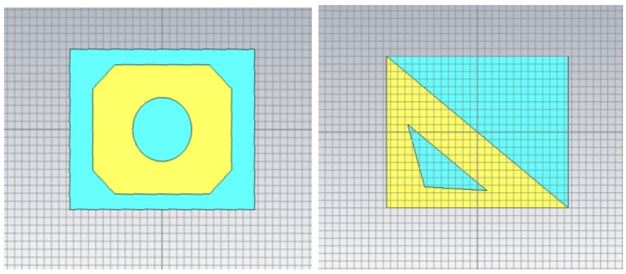

a) b)
Fig.2 Layout of the proposed antenna a) Front view b) Rear view [45]

III. PROPOSED RESEARCH DESIGN

The antenna designed in this research has been simulated with the help of Computer Simulation Technology (CST) 2022. The substrate used for the patch antenna is a textile material: “Felt” for its wearable purpose and biomedical purpose. The textile substrate chosen has a dielectric constant of 1.36 and a loss tangent (δ) of 0.023. For designing the suggested circular patch antenna, the equations used to determine its dimensions are as follows [46], [47]:

$$W = \frac{c}{2f_o\sqrt{\frac{(\varepsilon_r+1)}{2}}} \quad (1)$$

$$L_{eff} = \frac{c}{2f_o\sqrt{\varepsilon_{eff}}} \quad (2)$$

$$L = L_{eff} - 2\Delta L \quad (3)$$

$$R = ((L + (1.5 \times Dh))\times(W+(1.5\times Dh)))^{1/2})/2 \quad (4)$$

The suggested circular patch antenna resulted in having a Radius (R) of 20.264mm and height of 0.035mm. The designed antenna operates within the frequency range of 1-6 GHz also known as the Sub-6GHz and has a substrate height of 2.5mm.

The proposed antenna incorporates the feeding technique known as the "Proximity Coupling". In this technique, instead of having the feedline connected to the patch, it is placed between two layers of dielectric substrate and is electromagnetically coupled. The impedance matching of the antenna is 50 Ω. A Plus shaped slot is also cut on the patch to enhance its efficiency and improve on its radiation pattern and gain. The antenna design also comprises of a Defected Ground Structure (DGS) to increase the no. of bands and increase the total gain and bandwidth in the simulated results.

The final design of the patch antenna is presented as below in Fig.3 and 4 :

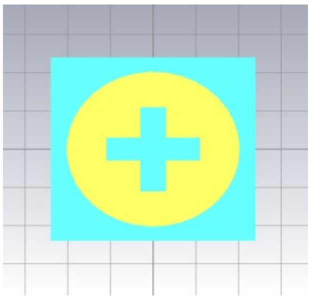

Fig.3 Proposed wearable Circular Patch antenna

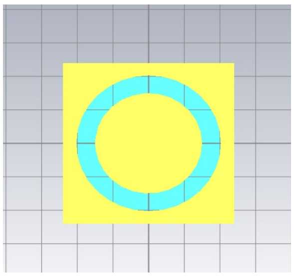

Fig.4 DGS of the Circular Patch antenna

The design parameters and specification of the wearable circular patch antenna are given in the following table (Table 1):

Table 1.
Specifications and parameters for the Wearable antenna

S.No	Description	Units
1.	Substrate Dielectric Constant	1.36
2.	Operating Frequency Range	1.0-6.0 GHz
3.	Input Impedance	50 Ω
4.	Substrate Width	48mm
5.	Substrate Length	48mm
6.	Substrate height	2.5mm
7.	Ground Width	48mm
8.	Ground Length	48mm
9.	Patch Radius	20.264mm
10.	Width of Feed line	2.82mm
11.	Length of Feed line	25.40mm

The research is further continued for the detection of Kidney Stones within the human body. To perform this task, a human body phantom has been created on which the patch antenna has been placed. The body phantom consists of 3 layers: Skin,Fat and Muscle. The figure below (Fig.5) shows the proposed antenna placed on a human body phantom.

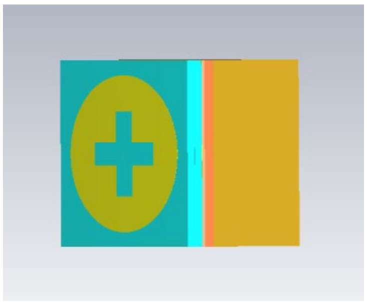

Fig.5 Proposed Antenna placed on human body phantom

The specifications for the body phantom are as presented in the tables (Table 2 and Table 3) below:

Table 2.
Specifications for the human body phantom

S.No	Description	Width (in mm)	Length (in mm)	Height (in mm)
1.	Skin	30	30	1
2.	Fat	30	30	3
3.	Muscle	30	30	30

Table 3
Dimensions of the human body phantom

S.No	Description	Dielectric constant	Loss tangent	Density
1.	Skin	7.98	1.37	1125 kg/m^3
2.	Fat	3.13	0.27	916 kg/m^3
3.	Muscle	12.86	0.0012	1084 kg/m^3

The suggested antenna is now placed in front of the body phantom designed representing a kidney and the stone within it as shown in Fig.6. The phantom created has two layers: Kidney and the stone within it for the detection. The specification of this phantom is presented in Table (Table 4) below:

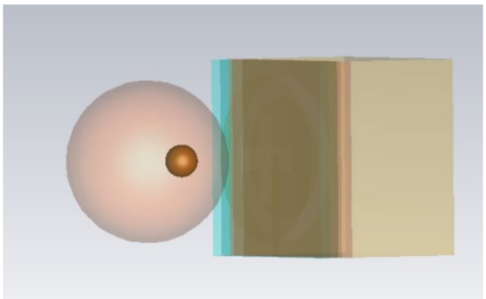

Fig.6 Proposed human body phantom for kidney stone detection

Table 4.
Specifications of the body phantom for tumour detection

S.No	Description	Dielectric constant	Loss tangent
1.	Kidney	98.1	0.811
2.	Kidney Stone	3.1	0.04

IV. DISCUSSION OF SIMULATED RESULTS

The simulated results of the suggested antenna is achieved and discussed within this section. The antenna is built on the substrate Felt and has made use of proximity coupling as its feeding technique with the help of CST Studio Suite 2022. The results obtained, proves that the antenna is operational and is useful for wearable and the detection of kidney stone. The achieved simulated results are presented and explained below:

A. On Free Space

The proposed antenna is foremost placed on free space and is presented previously in Fig.3 The antenna designed is also observed to be having two or dual bands. The simulated results for the antenna are presented and discussed below:

a) S_{11} Parameters

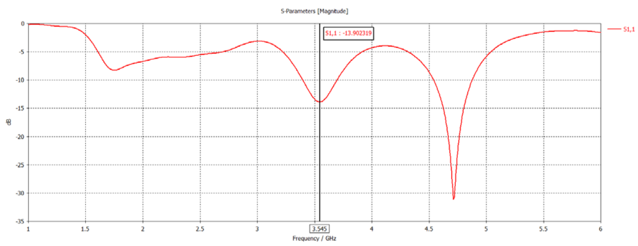

Fig.7 S_{11} parameters at 3.545 GHz

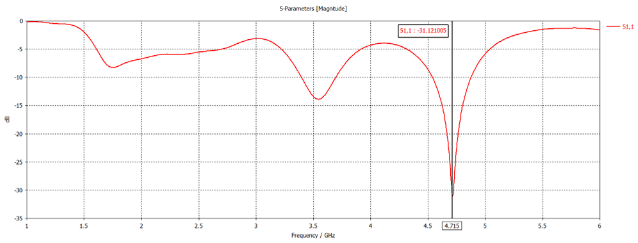

Fig.8 S_{11} parameters at 4.715 GHz

From Fig.7 and 8, the simulated results show that at resonating frequencies: 3.545 and 4.715 GHz, the S_{11} parameters obtained are: -13.902dB and -31.121 dB respectively.

b) VSWR

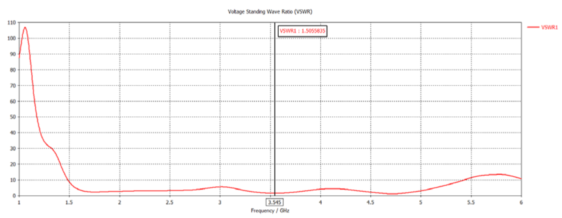

Fig.9 VSWR at 3.545 GHz

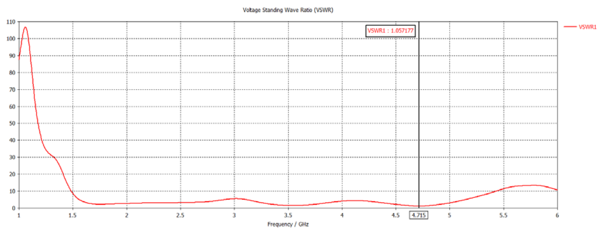

Fig.10 VSWR at 4.715 GHz

From Fig.9 and 10, the simulated results for VSWR at both the resonating frequencies 3.545 and 4.715GHz are 1.505 and 1.057 respectively.

c) Gain

From Fig.11 and 12, the simulated results at both frequencies 3.545 and 4.715GHz, the gain achieved is 5.792 dbi and 5.325 dbi respectively

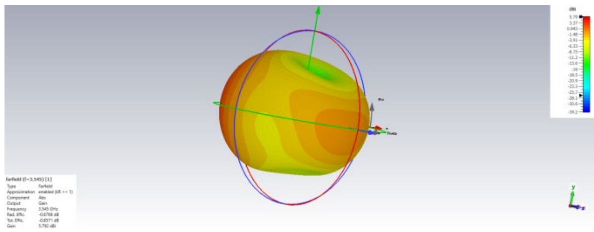

Fig.11 Gain at 3.545GHz

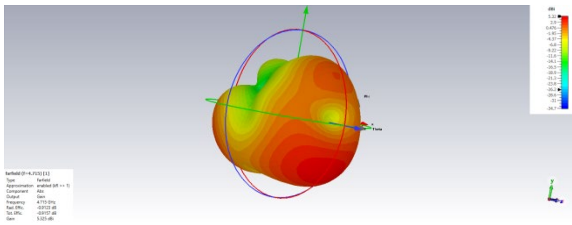

Fig.12 Gain at 4.715GHz

d) Directivity

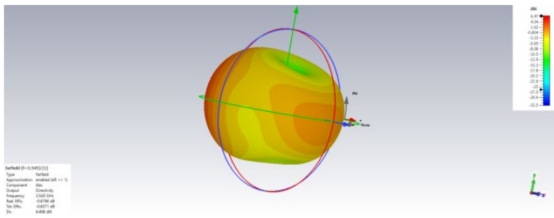

Fig.13 Directivity at 3.545GHz

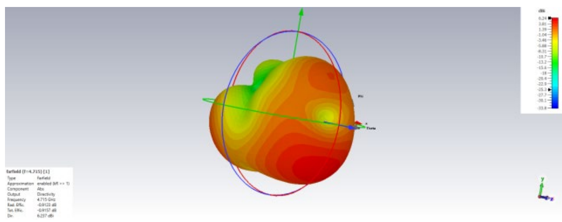

Fig.14 Directivity at 4.715GHz

From Fig.13 and 14 ,the results achieved at both the resonating frequencies of 3.545 and 4.715GHz, are 6.468 dbi and 6.236 dbi respectively

The simulation results on free-space are presented in a tabular format below (Table 5):

Table 5
Simulation results on Free-space

S.No.	Parameter	@3.545GHz	@4.715 GHz
1.	S11	-13.902 dB	-31.121 dB
2.	VSWR	1.505	1.057
3.	Gain	5.792 dbi	5.325 dbi
4.	Directivity	6.468 dBi	6.237 dBi

B. On Human body phantom

The human body phantom and its specification has been discussed in the previous section. This section discusses and presents the simulated results of the antenna when placed on the phantom. After simulation 3 resonant frequencies were achieved out of which the only acceptable frequency having acceptable results are at 2.715GHz. The results achieved are shown below along with their figures and table (Table 7).

a) S_{11} Parameters

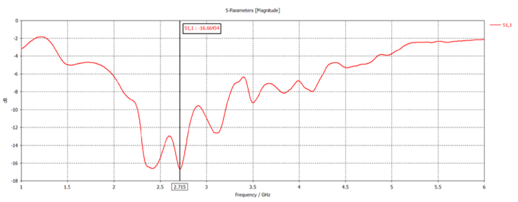

Fig15. S_{11} parameters at 2.715GHz

From Fig.15 ,the simulated results present that the S_{11} parameters achieved is -16.664 dB at 2.715GHz.

b) VSWR

From Fig.16 ,the simulated results present that the VSWR achieved is 1.344 at 2.715GHz.

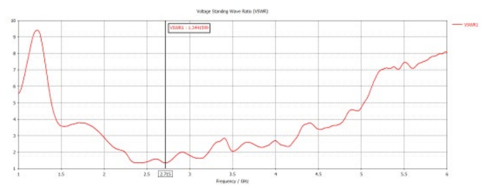

Fig.16 VSWR at 2.715GHz

c) Gain

From Fig.17 , the simulated results present that the gain achieved is 0.5684 dBi at 2.715GHz.

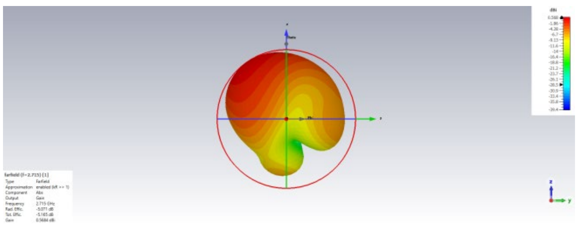

Fig.17 Gain at 2.715GHz

d) Directivity

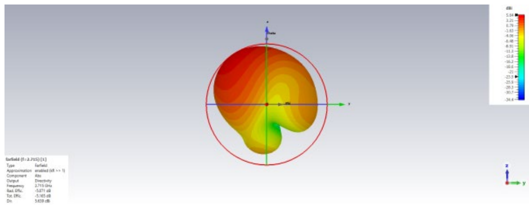

Fig.18 Directivity at 2.715GHz

From Fig.18 ,the simulated results present that the directivity achieved is 5.639 dBi at 2.715GHz.

Table 7
Simulation results on Human body phantom

S.No.	Parameter	@2.715 GHz
1	S_{11}	-16.664 dB
2	VSWR	1.344
3	Directivity	5.639 dBi
4	Gain	0.5684 dBi

The simulation to test the SAR rate/value is carried out to verify the safety of the radiation when applied to a human body after the results were obtained on a human body phantom. The SAR value of 1.54 W/kg was found at 10g of tissue at an input power of 60mW and 6.76 W/kg at 1g of tissue at the same input power. The below figure (Fig.19) presents the simulated SAR antenna result.

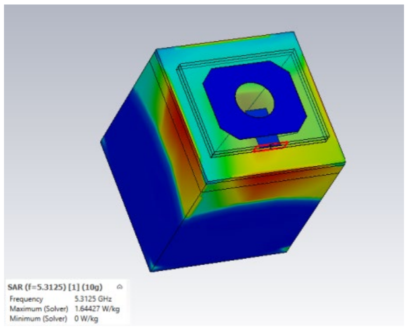

Fig.19 SAR of proposed antenna for 10g tissue

C. For Kidney Stone Detection

The suggested antenna has been designed for the detection of kidney stone for which a kidney stone phantom has been designed via CST Studio Suite 2022.(Fig.20).

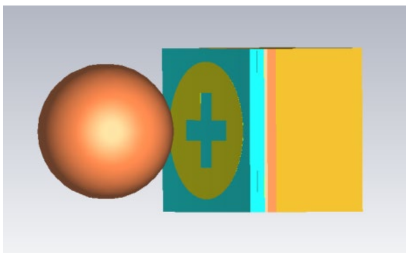

Fig.20 Human body phantom for kidney stone detection

The antenna was seen to be having 2 resonating frequencies: 2.745 GHz and 3.1 GHz.
The results for the simulated antenna are presented below along with figures and a table (Table 8):

a) S_{11} Parameters

From Fig.21, the simulated results presents the S_{11} parameters of -19.96 dB and -12.655 dB at 2.745GHz and 3.1GHz respectively.

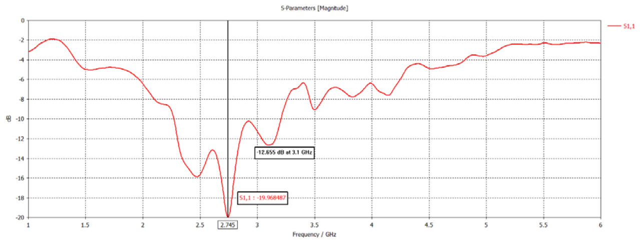

Fig.21 S_{11} parameters at 2.745 and 3.1GHz

b) VSWR

From Fig.22, the simulated results presents the achieved VSWR of 1.2 and 1.60 at frequencies 2.745 and 3.1GHz respectively.

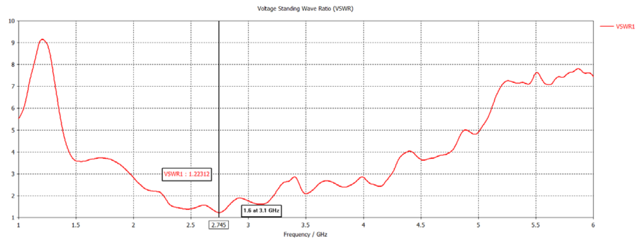

Fig.22 VSWR at 2.745 and 3.1GHz

c) Gain

From Fig.23 and 24, the results at the frequencies 2.745 and 3.1 GHz are 0.404 & -4.49 dBi respectively, which shows that the proposed antenna at the frequency 2.745GHz is suitable for kidney stone detection because of its suitable gain.

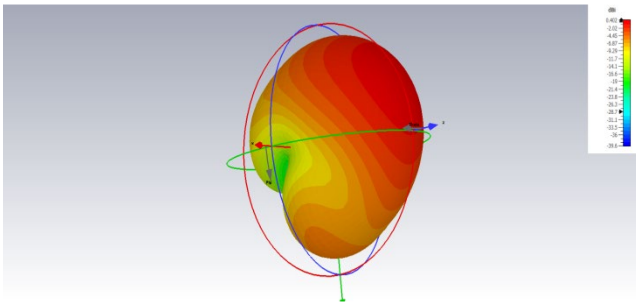

Fig.23 Gain at 2.745GHz

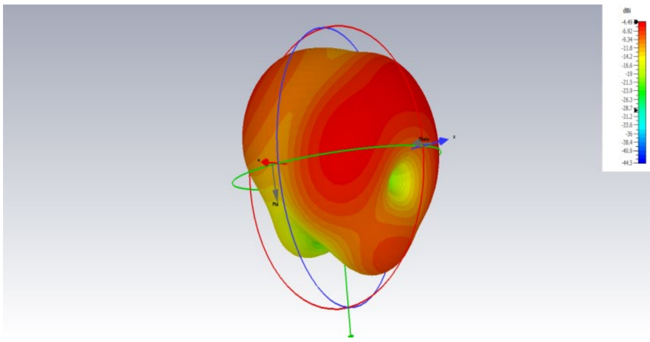

Fig.24 Gain at 3.1GHz

d) Directivity

From Fig.25 and 26, we can observe that at the operating frequency of 2.745GHz and 3.1 GHz, the directivity achieved is 5.98 and 4.53 dBi respectively.

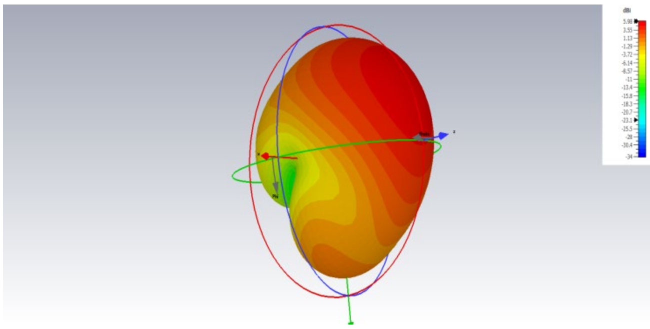

Fig.25 Directivity at 2.745GHz

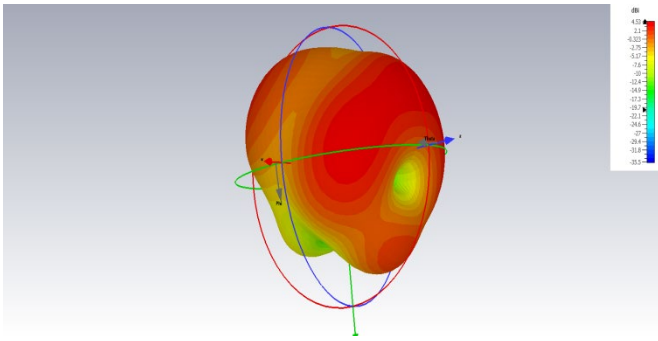

Fig.26 Directivity at 3.1GHz

Table 8
Simulation results for Kidney Stone Detection

S.No.	Parameter	@2.75 GHz	@3.1 GHz
1.	S_{11}	-21.325 dB	-12.580 dB
2.	Directivity	5.98 dBi	4.93 dBi
3.	VSWR	1.18	1.61
4.	Gain	0.404	-4.49 dBi

D. COMPARITIVE ANALYSIS

The table below (Table 9) has presented a comparison of results between previous research study done in the past few years.

Table 9
Comparative Analysis of Previous Study

Ref.	Year	Substrate	Resonant Frequency (GHz)	S11 (dB)	VSWR	Gain	SAR (W/kg)
[43]	2020	FR-4	2.424	-22.299	--	--	0.540
[42]	2020	Jeans	4.5 & 8.75	-44.25 (at 8.75 GHz)	1.01	3.01 dB	--
[44]	2021	Rogers 3210	915MHz & 2.45	-23.0 (at 2.45 GHz)	< 2.0	--	32 (at 0.5W)
[45]	2024	Cotton	5.11 & 7.39	-46.058 (at 5.11 GHz)	1.010	4.204 dBi	1.64 (at 30mW)
Proposed work	2024	Felt	3.545 & 4.715	-13.902 & -31.121 (at 3.545 & 4.715)	1.50 & 1.05	5.792 dBi & 5.325 dBi	1.54 (at 60mW)

V. FUTURE SCOPE

There still exists a lot of potential in improving and designing microstrip patch antennas having different frequency ranges and other textile substrates which can enhance the achieved gain and efficiency of the antenna.

Techniques such as mentioned below can also help in increasing the results, they are as such:

1) Use of Metamaterials
2) Designing AMC Structures.
3) Incorporating EBG Structures etc.

These techniques can help increase the gain and bandwidth of the patch antenna for a range of uses. The antenna's SAR value may be further decreased by implementing these technologies. Because they are inexpensive and portable, microstrip patch antennas are widely utilized in a variety of fields, including biomedicine, where they are useful for kidney stone detection, medical imaging, tumor detection,and other applications [37]-[39].

The parameters/dimensions proposed in this research can possibly achieve enhanced results by changing the size or shape of the patch or slots, or having a DGS of a different shape. The substrate chosen can also be chosen on the basis of lower dielectric constants than used in this study [51], [52].

VI. CONCLUSION

The research proposes and has successfully designed a wearable circular patch antenna within the Sub-6GHz frequency range for kidney stone detection via the help of CST Studio Suite 2022. The antenna is dual band in nature and has an overall size of $48x48x5mm^3$. The feeding technique used in the study is the proximity coupled feeding than the commonly used microstrip line feeding.The suggested antenna has been also tested to be wearable by

n a designed human body phantom. so proved to be used for the detection of kidney stones within the human body by designing a body phantom of the human kidney.

The antenna designed achieved a -13.902 dB return loss, a VSWR of 1.50 and a directivity of 6.468 dBi at 3.545GHz and a -31.121 dB return loss, a VSWR of 1.057, and a directivity of 6.237 dBi at 4.715GHz when placed on free-space. A gain of 5.792 dBi and 5.325 dBi was obtained at 3.545GHz and 4.715GHz respectively. When placed on a body phantom, the gain achieved was only 0.568 dBi at 2.715GHz and a gain of 0.404 dBi at 2.745GHz when placed in front of kidney stone phantom.

It also achieved a SAR value of 1.54 W/kg for a 10g tissue with an input power of only 60mW which proves its safety and performance for biomedical applications.

The primary goal of this study is to create and simulate an antenna which could be used for any biomedical application such as kidney stone or tumour detection and can also be functional as a wearable patch antenna or on free-space. The achieved results further prove that the proposed wearable antenna consists of a high gain, suitable VSWR and is also having SAR value as low as 1.54 W/kg which is not harmful to the human body.

REFERENCES

[1] P. M. Potey and K. Tuckley, "Design of wearable textile antenna with various substrate and investigation on fabric selection," in *2018 3rd International Conference on Microwave and Photonics (ICMAP)*, IEEE, Feb. 2018, pp. 1–2. doi: 10.1109/ICMAP.2018.8354539.

[2] B. Roy, A. K. Bhatterchya, and S. K. Choudhury, "Characterization of textile substrate to design a textile antenna," in *2013 International Conference on Microwave and Photonics (ICMAP)*, IEEE, Dec. 2013, pp. 1–5. doi: 10.1109/ICMAP.2013.6733490.

[3] D. Ferreira, P. Pires, R. Rodrigues, and R. F. S. Caldeirinha, "Wearable Textile Antennas: Examining the effect of bending on their performance," *IEEE Antennas Propag Mag*, vol. 59,

no. 3, pp. 54–59, Jun. 2017, doi: 10.1109/MAP.2017.2686093.

[4] P. M. Potey and K. Tuckley, "Design of wearable textile antenna for low back radiation," *J Electromagn Waves Appl*, vol. 34, no. 2, pp. 235–245, Jan. 2020, doi: 10.1080/09205071.2019.1699170.

[5] V. K. Singh, M. Chaudhary, A. Yadav, V. K. Singh, and H. Mohan, "A Review on Wearable Textile Antenna Journal of Telecommunication, Switching Systems and Networks A Review on Wearable Textile Antenna," 2015. [Online]. Available: www.stmjournals.com

[6] A. Roy, A. K. Biswas, A. Nandi, and B. Basu, "Ultra-Wideband Flexible Wearable Antenna with Notch Characteristics for WLAN Applications," 2023.

[7] P. Nigam, K. Goyal Jyoti Electronics, B. Raj Dutta, Mt. Scholar, and K. Goyal Associate Member, *W-Band Filter for Satellite Application*. 2017. [Online]. Available: https://www.researchgate.net/publication/329442655

[8] A. Kumar, B. Raj, D. #2, and S. Budhauliya, "Iterated Pythagorean Fractal Tree Multiband Antenna," *International Journal of Scientific and Research Publications*, vol. 3, no. 9, 2013, [Online]. Available: www.ijsrp.org

[9] D. Shukla, B. R. Dutta, and B. K. Kanaujia, "Design of microwave imaging based microstrip ultra-wideband antenna," in *2015 Annual IEEE India Conference (INDICON)*, IEEE, Dec. 2015, pp. 1–5. doi: 10.1109/INDICON.2015.7443760.

[10] A. Y. I. Ashyap *et al.*, "Inverted E-Shaped Wearable Textile Antenna for Medical Applications," *IEEE Access*, vol. 6, pp. 35214–35222, 2018, doi: 10.1109/ACCESS.2018.2847280.

[11] Juan Wen, Danpeng Xie, Xueguan Liu, Huiping Guo, Changrong Liu, and Xinmi Yang, "Wideband collar-shaped antenna for RF energy harvesting," in *2016 Asia-Pacific International Symposium on Electromagnetic Compatibility (APEMC)*, IEEE, May 2016, pp. 253–255. doi: 10.1109/APEMC.2016.7523025.

[12] B. Pham, J.-C. S. Chieh, and A.-V. Pham, "A wideband composite right/left hand rectenna for UHF energy harvesting applications," in *Proceedings of the 2012 IEEE International Symposium on Antennas and Propagation*, IEEE, Jul. 2012, pp. 1–2. doi: 10.1109/APS.2012.6349186.

[13] M. Khan and B. R. Dutta, "A Square Loop Frequency Selective Surface for Designing Secure Electromagnetic Buildings," in *2016 International Conference on Micro-Electronics and Telecommunication Engineering (ICMETE)*, IEEE, Sep. 2016, pp. 23–27. doi: 10.1109/ICMETE.2016.15.

[14] B. R. Dutta, B. K. Kanaujia, and C. Dalela, "Elliptical BandPassThree Dimensional Frequency Selective Surface with Multiple Transmission Zeros," *Indonesian Journal of Electrical Engineering and Computer Science*, vol. 12, no. 3, p. 1020, Dec. 2018, doi: 10.11591/ijeecs.v12.i3.pp1020-1029.

[15] B. R. Dutta, B. K. Kanaujia, and C. Dalela, "3D FSS with multiple transmission zeros and pseudo elliptic response," *Bulletin of Electrical Engineering and Informatics*, vol. 8, no. 3, pp. 923–932, Sep. 2019, doi: 10.11591/eei.v8i3.1292.

[16] B. R. Dutta, R. Chaudhury, A. Tripathi, and B. Biswas, "ADVANCE T-SHAPED MICROSTRIP PATCH ANTENNA FOR IMPROVED RADIO FREQUENCY ENERGY HARVESTING," *Telecommunications and Radio Engineering*, vol. 83, no. 1, pp. 1–16, 2024, doi: 10.1615/TelecomRadEng.2023049976.

[17] B. R. Dutta *et al.*, "Advance 3D FSS with several transmission zeros for S, C and X frequency," *Mater Today Proc*, vol. 74, pp. 314–323, 2023, doi: 10.1016/j.matpr.2022.08.251.

[18] M. Parmar, L. Gupta, and B. R. Dutta, "Storage Optimized Secured Data Transaction of IoT Sensors," in *2022 IEEE 2nd International Conference on Mobile Networks and Wireless Communications (ICMNWC)*, IEEE, Dec. 2022, pp. 1–6. doi: 10.1109/ICMNWC56175.2022.10031866.

[19] R. Bansal and B. R. Dutta, "An Optimize Approach to Reduce Uncertainties in WDM Networks," 2023, pp. 601–612. doi: 10.1007/978-981-19-9638-2_52.

[20] R. Yadav, B. R. Dutta, S. K. Mishra, A. K. Johar, and A. Tripathi, "3D MIMO beam forming using machine learning SVM algorithm for 5G wireless communication network," 2023, p. 020018. doi: 10.1063/5.0154165.

[21] R. Chaudhury and B. R. Dutta, "Advance Antenna Array Design for Sub-6GHz 5G applications," in *2023 14th International Conference on Computing Communication and Networking Technologies (ICCCNT)*, IEEE, Jul. 2023, pp. 1–10. doi: 10.1109/ICCCNT56998.2023.10308217.

[22] D. M. John, S. Vincent, S. Pathan, P. Kumar, and T. Ali, "Flexible Antennas for a Sub-6 GHz 5G Band: A Comprehensive Review," *Sensors*, vol. 22, no. 19, p. 7615, Oct. 2022, doi: 10.3390/s22197615.

[23] S. Kumar, A. S. Dixit, R. R. Malekar, H. D. Raut, and L. K. Shevada, "Fifth Generation Antennas: A Comprehensive Review of Design and Performance Enhancement Techniques," *IEEE Access*, vol. 8, pp. 163568–163593, 2020, doi: 10.1109/ACCESS.2020.3020952.

[24] C.-Y.-D. Sim, H.-Y. Liu, and C.-J. Huang, "Wideband MIMO Antenna Array Design for Future Mobile Devices Operating in the 5G NR Frequency Bands n77/n78/n79 and LTE Band 46," *IEEE Antennas Wirel Propag Lett*, vol. 19, no. 1, pp. 74–78, Jan. 2020, doi: 10.1109/LAWP.2019.2953334.

[25] M. Agiwal, A. Roy, and N. Saxena, "Next Generation 5G Wireless Networks: A Comprehensive Survey," *IEEE Communications Surveys & Tutorials*, vol. 18, no. 3, pp. 1617–1655, 2016, doi: 10.1109/COMST.2016.2532458.

[26] Md. A. Sufian, N. Hussain, H. Askari, S. G. Park, K. S. Shin, and N. Kim, "Isolation Enhancement of a Metasurface-Based MIMO Antenna Using Slots and Shorting Pins," *IEEE Access*, vol. 9, pp. 73533–73543, 2021, doi: 10.1109/ACCESS.2021.3079965.

[27] A. Iqbal *et al.*, "Electromagnetic Bandgap Backed Millimeter-Wave MIMO Antenna for Wearable Applications," *IEEE Access*, vol. 7, pp. 111135–111144, 2019, doi: 10.1109/ACCESS.2019.2933913.

[28] B. R. Dutta and B. Biswas, "Review of Synergistic Integration of Microstrip Patch Antennas in Biomedical and Artificial Intelligence Domains," 2024, pp. 65–81. doi: 10.1007/978-3-031-54162-9_5.

[29] Al-Gburi, Ahmed Jamall Abdullah, Imran Ibrahim, and Zahriladha Zakaria, "A miniature raspberry shaped UWB monopole antenna based on microwave imaging scanning technique for kidney stone early detection," *Int. J. Psychosoc. Rehabil* , vol. 24, no. 2, pp. 1755–1763, 2020.

[30] D. A. Saleeb, R. M. Helmy, N. F. F. Areed, M. Marey, K. M. Almustafa, and A. S. Elkorany, "Detection of Kidney Cancer Using Circularly Polarized Patch Antenna Array," *IEEE Access*, vol. 10, pp. 78102–78113, 2022, doi: 10.1109/ACCESS.2022.3192555.

[31] M. A. Salim, "THE VARIATIONS IN DIELECTRIC PROPERTIES OF CALCIUM OXALATE MONOHYDRATE SINGLE CRYSTALS DUE TO DOPING OF IMPURITIES," 2011.

[32] D. Sinha *et al.*, "Studies on the dielectric properties of natural urinary stones," in *Advanced Materials Research*, 2012, pp. 484–488. doi: 10.4028/www.scientific.net/AMR.584.484.

[33] T. Rahman and M. S. Uddin, "Speckle noise reduction and segmentation of kidney regions from ultrasound image," in *2013 International Conference on Informatics, Electronics and Vision (ICIEV)*, IEEE, May 2013, pp. 1–5. doi: 10.1109/ICIEV.2013.6572601.

[34] Mohamad ALWAN and Sawsan SADEK, "Investigation of Kidney Stone Using a Microstrip Patch Antenna Scanning System," *Journal of Diagnostics*, vol. 3, no. 1, pp. 1–10, 2016.

[35] H. Zhang, M. Ren, Y. Wang, and H. Qin, "A high-efficient excitation-detection thermoacoustic imaging probe for breast tumor detection," *Med Phys*, vol. 50, no. 3, pp. 1670–1679, Mar. 2023, doi: 10.1002/mp.16179.

[36] D. A. Saleeb, R. M. Helmy, N. F. F. Areed, M. Marey, K. M. Almustafa, and A. S. Elkorany, "Detection of Kidney Cancer Using Circularly Polarized Patch Antenna Array," *IEEE Access*, vol. 10, pp. 78102–78113, 2022, doi: 10.1109/ACCESS.2022.3192555.

[37] K. Viswanath and R. Gunasundari, "Design and analysis performance of kidney stone detection from ultrasound image by level set segmentation and ANN classification," in *2014 International Conference on Advances in Computing, Communications and Informatics (ICACCI)*, IEEE, Sep. 2014, pp. 407–414. doi: 10.1109/ICACCI.2014.6968485.

[38] W. M. Hafizah, E. Supriyanto, and J. Yunus, "Feature Extraction of Kidney Ultrasound Images Based on Intensity Histogram and Gray Level Co-occurrence Matrix," in *2012 Sixth Asia Modelling Symposium*, IEEE, May 2012, pp. 115–120. doi: 10.1109/AMS.2012.47.

[39] B. Borja, J. A. Tirado-Mendez, and H. Jardon-Aguilar, "AN OVERVIEW OF UWB ANTENNAS FOR MICROWAVE IMAGING SYSTEMS FOR CANCER DETECTION PURPOSES," *Progress In Electromagnetics Research B*, vol. 80, pp. 173–198, 2018, doi: 10.2528/PIERB18030302.

[40] S. Rao, A. Singh, A. K. Bhat, and R. Shetty, "Tumor Detection Using Microstrip Patch Antenna Operating in FCC MBAN Band," *Progress In Electromagnetics Research C*, vol. 136, pp. 215–227, 2023, doi: 10.2528/PIERC23070103.

[41] F. Mahbub and R. Islam, "Performance Analysis of a Cylindrical Dielectric Resonator Antenna (CDRA) for the Detection of Early-Stage Stones of the Human Kidney," in *2022 Workshop on Microwave Theory and Techniques in Wireless Communications (MTTW)*, IEEE, Oct. 2022, pp. 123–128. doi: 10.1109/MTTW56973.2022.9942519.

[42] P. Kumar, S. · Sławomir, T. Wierzchoń, S. Tanwar, M. Ganzha, and J. J. P. C. Rodrigues, "Lecture Notes in Networks and Systems 203 Proceedings of Second International Conference on Computing, Communications, and Cyber-Security," 2020. [Online]. Available: http://www.springer.com/series/15179

[43] S. Sinha, T.-S. R. Niloy, R. R. Hasan, Md. A. Rahman, and S. Rahman, "A Wearable Microstrip Patch Antenna for Detecting Brain Tumor," in *2020 International Conference on Computation, Automation and Knowledge Management (ICCAKM)*, IEEE, Jan. 2020, pp. 85–89. doi: 10.1109/ICCAKM46823.2020.9051494.

[44] A. Z. A. Zaki, T. G. Abouelnaga, E. K. I. Hamad, and H. A. Elsadek, "Design of dual-band implanted patch antenna system for bio-medical applications," *Journal of Electrical Engineering*, vol. 72, no. 4, pp. 240–248, Aug. 2021, doi: 10.2478/jee-2021-0033.

[45] R. Chaudhury and B. R. Dutta, "Advanced Ultrawideband Patch Antenna for Wearable and WBAN Applications," *Telecommunications and Radio Engineering*, 2024, doi: 10.1615/TelecomRadEng.2024051936.

[46] P. K. S. M. and B. A. T. P. Puttaswamy, "Analysis of loss tangent effect on Microstrip antenna gain," *International Journal of Applied Sciences and Engineering Research*, vol. 3, no. 6, pp. 1102–1107, 2014.

[47] G. George, R. Nagarjun, D. Thiripurasundari, R. Poonkuzhali, and Z. C. Alex, "Design of meander line wearable antenna," in *2013 IEEE CONFERENCE ON INFORMATION AND COMMUNICATION TECHNOLOGIES*, IEEE,

Apr. 2013, pp. 1190–1193. doi: 10.1109/CICT.2013.6558281.

[48] K. Jayabharathy and T. Shanmuganantham, “Design of a Compact Textile Wideband Antenna for Smart Clothing,” in *2019 2nd International Conference on Intelligent Computing, Instrumentation and Control Technologies (ICICICT)*, IEEE, Jul. 2019, pp. 477–481. doi: 10.1109/ICICICT46008.2019.8993388.

[49] B. Gupta, S. Sankaralingam, and S. Dhar, “Development of wearable and implantable antennas in the last decade: A review,” in *2010 10th Mediterranean Microwave Symposium*, IEEE, Aug. 2010, pp. 251–267. doi: 10.1109/MMW.2010.5605178.

[50] S.-H. Li and J. Li, “Smart patch wearable antenna on Jeans textile for body wireless communication,” in *2018 12th International Symposium on Antennas, Propagation and EM Theory (ISAPE)*, IEEE, Dec. 2018, pp. 1–4. doi: 10.1109/ISAPE.2018.8634084.

[51] M. Turkmen and H. Yalduz, “Design and Performance Analysis of a Flexible UWB Wearable Textile Antenna on Jeans Substrate,” *International Journal of Information and Electronics Engineering*, vol. 8, no. 2, pp. 15–18, Jun. 2018, doi: 10.18178/IJIEE.2018.8.2.687.

[52] R. Chaudhury and B. Raj Dutta, “Design Analysis on Wearable Patch Antenna for Wireless Applications,” *GRENZE International Journal of Engineering and Technology*, vol. 10, no. 1, pp. 273–283, 2024.